MATCH
Communications in Mathematical and in Computer Chemistry

MATCH Commun. Math. Comput. Chem. **94** (2025) 863–889
ISSN: 0340–6253
doi: 10.46793/match.94-3.09225

Impact of Hopf and Bautin Bifurcations on an Autocatalytic Chemical Reaction System

Xing Gao, Yinlai Jin, Muhammad Marwan*, Feng Li, Yunlan Wei*

School of Mathematics and Statistics, Linyi University, Linyi 276005, Shandong, China

gxing2025@163.com, jinyinlai@lyu.edu.cn, marwan78642@zjnu.edu.cn, lifeng@lyu.edu.cn, wyl19910110@163.com

(Received April 21, 2025)

Abstract

In this paper, we discuss the influence of mathematical computations i.e. codimension one and codimension two bifurcations on an autocatalytic chemical system. In the past, it was shown that the considered dynamical system exhibits Hopf bifurcation on the positive equilibria, but in current study we have symbolically identified that the study of bifurcation in this dynamical system is not limited to Hopf bifurcation. For this purpose, a complete chart of eigenvalues for the stability of autocatalytic reaction system is provided that shows that equilibrium points E_3 and P have the possibility of other type of bifurcations. Mathematically, the first Lyapunov coefficient is used to determine the type of Hopf bifurcation and is extended to second Lyapunov coefficient for the possibility of Bautin bifurcation, whereas the provided analytical results are theoretical analyzed and physical interpreted to further explore the dynamics of autocatalytic chemical reaction dynamical system in various parametric regions. It is shown that how the balancing of two reactions behave between steady and oscillatory states. Similarly, the Bautin

*Muhammad Marwan and Yunlan Wei are corresponding authors

bifurcation identify severe sensitive transition in various oscillatory regimes, where their corresponding unfolding parameters scales the transition between different oscillatory states. Finally, MATLAB is used to simulate not only the analytical results for the qualitative analysis of trajectories around equilibrium points but also to easily understand the discussed physical meaning of provided mathematical results.

Introduction

The reactions taking place in chemistry follows several rules including balancing that in response can follow the rule of dynamics. Recent years have seen growing interest in studying the unpredictable dynamics of nonlinear systems using theoretical analysis and computational modeling. Beyond the fundamental question of how molecular-scale interactions give rise to organized large-scale behavior, these methods allow researchers to evaluate conceptual models against real-world observations. Furthermore, such studies can guide experimental work by identifying measurable phenomena worth exploring.

Chaotic phenomena in a well-stirred chemical systems [1] provide a way to generate chaos in intrinsic nonlinearities instead of spatial degrees of freedom and elaborate a way to provide a bridging passage between microscopic and macroscopic behaviors. The process in which the balancing of equations are transformed into a chemical mechanism is considered as a suitable choice for the investigation of dynamical attitude at microscopic aspect in systems demonstrating bifurcation and chaos.

In 2018, a discrete system showing the dioxide-iodine-malonic acid chemical reactions was considered to study Neimark-Sacker bifurcation and its control using feedback and hybrid control methods [2]. An autocatalator chemical reaction system is converted into fractional order using Caputo derivative, and its codimension-one and codimension-two bifurcations are discussed using bifurcation diagram and normal form theory [3]. Chen provided deep analysis of a modified Brusselator system in 2023 by studying Hopf bifurcation along with its type using the first Lyapunov coefficient and self-organization patterns [4]. Recently, Khan et al [5] investigated the dynamics of a modified Brusselator system using codimension-one and codimension-two bifurcations linked with strong resonances.

Several dynamical systems of ordinary differential equations (ODEs) have been designed and studied on the bases of chemical reactions including two-species model [6], smallest chemical reaction system [7], autocatalytic glycolysis [8], Belousov-Zhabotinsky [9], cubic autocatalator [10] oregonator [11], enzyme-catalyzed [12], Degn-Harrison reaction [13] but the system that we have considered in this paper is an autocatalytic chemical reaction-based, well-stirred chemicals, and is famous as Williamowski Rossler (WR) [1];

$$\begin{cases} \dot{x} = ax - bx^2 - xy - xz, \\ \dot{y} = xy - cy, \\ \dot{z} = dz - xz - \alpha z^2, \end{cases} \tag{1}$$

where $(x,\, y,\, z)$ are state variables of system (1) and $(a,\, b,\, c,\, d,\, \alpha) \in \mathbb{R}^5$ are parameter values. System (1) is obtained by non-dimensionalizng the parameters, $a = k_1\,[\mathrm{A}_1]$, $b = k_{\bar{1}}$, $c = k_5\,[\mathrm{A}_5]$, $d = k_4\,[\mathrm{A}_4]$, and $\alpha = k_{\bar{5}}$ given in the following chemical reactions†

$$\begin{aligned} &A_1 + X \underset{k_{\bar{1}}}{\overset{k_1}{\rightleftharpoons}} 2X, \quad X + Y \underset{k_{\bar{2}}}{\overset{k_2}{\rightleftharpoons}} 2Y, \\ &A_5 + Y \underset{k_{\bar{3}}}{\overset{k_3}{\rightleftharpoons}} A_2, \quad X + Z \underset{k_{\bar{4}}}{\overset{k_4}{\rightleftharpoons}} A_3, \\ &A_4 + Z \underset{k_{\bar{5}}}{\overset{k_5}{\rightleftharpoons}} 2Z, \end{aligned} \tag{2}$$

that rely on double auto-catalytic steps by coupling the ingredients X and Z with three other steps including the third constitute Y. Moreover, $(A_1,\, A_4,\, A_5)$ the initials and $(A_2,\, A_3)$ final product concentrations are kept fixed. The constants $k_{\pm i}, i = 1, \ldots, 5$ are additional points that are parameterized to obtain the parameters given in the system (1) and need to be specified accordingly for the desired study.

The mathematical literature related to the WR system is traced back from the work of Gysermans and Nicolis [14], where this system was an-

†It is important to mention that, $k_{\bar{1}} = k_{-1}$ and similarly other as well.

alyzed with the help of stochastic theory. In 2005, Huang and Yan [15] discussed the existence of chaos in it along with some other properties. Xu and Wu added the time delayed term in WR system to not only discuss its bifurcation phenomenon but also discussed its stability in trajectories [16]. Gaspard [17] used stochastic analysis, where entropy is used as a tool to enhance the study of limit cycles in the considered system. Apart from this, the WR system was transformed into fractional order [18], where a synchronization technique was employed to visualize its importance in secure communication, whereas the same system using Caputo fractional derivatives and its control using adaptive-sliding technique [19] and PID controller [20] in 2022. The study related to its bounds using Lyapunov functions and oscillatory solutions, without considering eigenvalues, is discussed in the work of Din [1]. In 2022, the dynamics of WR system is classified according to local and global asymptotic stability of the solutions [22]. Moreover, the study related to its numerical bifurcation analysis and anti-control in a fractional order form is elaborated by Liu [23], while its complex dynamics along with synchronization techniques is analyzed in 2023 [24].

The qualitative study in which an equilibrium point can be created, vanished or changed its nature of stability with the changing in its parameter value is called bifurcation, whereas the parameter due to which such type of changes occur is called bifurcation parameter. Although, there are several types of well-known bifurcations [33, 34] but Hopf bifurcation [36, 37] has got much importance among them due to the existence of first limit cycle. In 1982, Hassard *et al.* [38] developed a technique for Hopf bifurcation that latter on got fame as normal form (NF) technique. In 2012, Wu et al. [39] derived normal form of Hopf bifurcation in rössler system, whereas recently Li *et al.* adopted the same technique for finding Hopf bifurcation along with its periodic limit cycle in a mechanical dynamical system [40]. The application of Hopf bifurcation with other dynamical properties such as Spatiotemporal oscillations and pattern formation in an Enzyme-Catalyzed reaction system are discussed by Chen *et al.* [31] and Zhao *et al.* [32].

Similarly, an analytical technique, the first Lyapunov coefficient, developed by Kuznetsov [41] got fame due to ease in finding type of Hopf bifurcation. Since then, several researchers used it in variety of real-life-based application models [42–44]. Apart from the usage of first Lyapunov coefficient in determining type of Hopf bifurcation, it plays vital role in the investigation of Bautin bifurcation at their critical points. Yang *et al.* [45] in 2008 worked on the two neuron-based systems by deriving its normal form to study bautin bifurcation. In the field of engineering, Inozemtsev *et al.* [46] considered a railway wheel-set system to explore conditions for bautin bifurcation with the aid of first Lyapunov coefficient. In 2012, a complete study of codimension two bifurcations including bautin bifurcation was provided in a two-dimensional Hindmarsh-rose model [47]. This bifurcation is not only limited to mathematical perspectives but had showed a glimpse of importance in ecology [48] as well.

The cited work in our paper discusses the importance of system (1), highlighting its applications in dynamical systems. However, the following points demonstrate the novelty of the current manuscript

(1) New stability and bifurcation regimes are explored in autocatalytic chemical reaction system to expand its dynamical analysis.

(2) Hopf bifurcation and its type are discussed for the equilibrium points E_3 and P using the first Lyapunov coefficient in system (1).

(3) Analytical criteria for the Bautin (generalized Hopf) bifurcation are derived using the second Lyapunov coefficient, revealing sensitive transitions between stable and unstable oscillatory regimes.

(4) Detailed bifurcation diagrams and their corresponding Lyapunov coefficients are shown, providing deeper insights into the system's dynamical behavior near critical bifurcation thresholds.

Mathematically, the first Lyapunov coefficient technique [41] is used for the computation of supercritical Hopf and Bautin bifurcations, whereas for chemical relevance, we linked the bifurcation parameters to reaction kinetics, showing how changing into parameter values can induce large-scale behavioral shifts such as chaos to limit cycles.

The subsequent sections are structured as follows. In section (1), a quick description about the equilibrium points, dynamics of trajectories around their equilibrium points and its chaotic attitude is given. A detailed analytical and qualitative analysis of the considered chemical system at E_3 and the positive equilibria in subsections (2.1) and (2.2) respectively are discussed. Finally, the concluding remarks are given in section (3).

1 Equilibrium points, local dynamics and chaos in autocatalytic chemical reaction system

The considered system (1) based on chemical reactions (2) has six equilibrium points: $O(0,0,0)$, $E_1(0,0,\frac{d}{\alpha})$, $E_2(\frac{a}{b},0,0)$, $E_3(c,a-bc,0)$, $E_4(\frac{d-a\alpha}{1-b\alpha},0,\frac{a-bd}{1-b\alpha})$, and $P(c,a-bc+\frac{c-d}{\alpha},\frac{d-c}{\alpha})$. In [21], it was calculated that the Hopf bifurcation in this system occur only at the positive equilibria, whereas around all other remaining equilibrium points trajectories show local dynamical behavior. It was further discussed that origin O is unstable node,

EP	Eigenvalues	Stability
O	$a,-b,d$	Unstable
E_1	$a-\frac{d}{\alpha},-c,-d$	Stable if $\alpha a < d$, Unstable if $\alpha a > d$
E_2	$-a,\frac{a-bc}{b},\frac{bd-a}{b}$	Stable if $bd < a < bc$, Unstable if $a > bc$ or $bd > a$
E_3	-	Stable if $d < c$, Unstable if $d > c$
E_4	-	Stable if $\frac{d-a\alpha}{1-b\alpha} < c$, Unstable if $\frac{d-a\alpha}{1-b\alpha} > c$

Table 1. Stability of equilibrium points based on eigenvalues [21]

while E_1 is stable (unstable) for $a\alpha < (>)d$. Similarly, E_2, E_3 and E_4 were shown stable and unstable respectively for their corresponding parametric adjustments given in Table 1.

Authors in [21] have also discussed the possibility of Hopf bifurcation for the unique positive equilibria; P without using their eigenvalues. Figure 1 is the bifurcation diagram and their corresponding Lyapunov exponents of system (1) in which the parameters a, b, c, d are kept fixed, whereas the topological dynamics of the considered system for different values of α are observed. For convenience, the phase portraits for various values

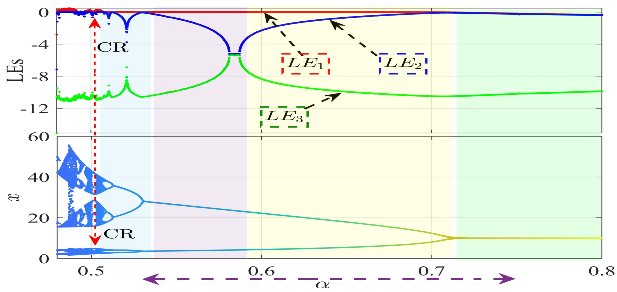

Figure 1. Bifurcation diagram and Lyapunov exponents of system (1) showing chaos for the variations in α.

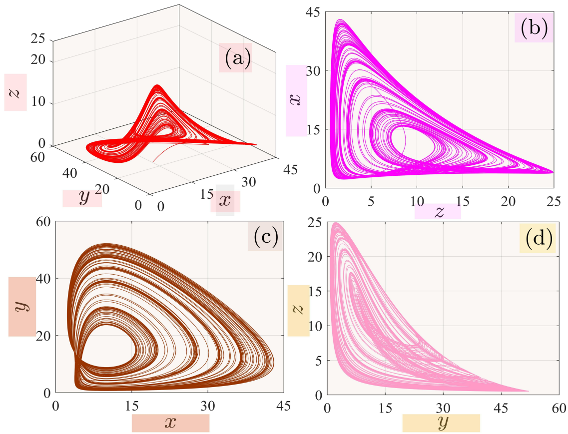

Figure 2. The three-dimensional phase portrait and various two-dimensional projections of the well-stirred chaotic system: (a) the $x_1 - x_2 - x_3$ space (b) the $x_1 - x_2$ plane (c) the $x_2 - x_3$ plane (d) the $x_1 - x_3$ plane.

of the parameter α are plotted. The Lyapunov exponents at the chaotic region (CR) are positive, zero and negative are illustrated in Fig. 1 at which the 3D phase portrait and 2D projections are shown in Fig. 2. The chaotic attitude in the trajectories of system (1) are observed at macroscopic level for the parameter values $a = 30$, $b = 0.415$, $c = 10$, $d = 16.5$, and $\alpha = 0.5$ with initial conditions (x_0, y_0, z_0)=(4, 5, 6), whereas the phase portraits for α in other regions are observed in Fig. 3. In the first region for $\alpha = 0.53$, high oscillations are seen that showed reduction in the second, third and fourth region for $\alpha = 0.57$, $\alpha = 0.65$ and $\alpha = 0.75$, respectively. Furthermore, each equilibrium point shows different topol-

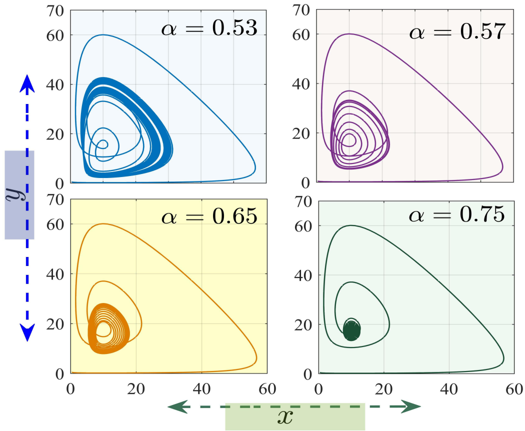

Figure 3. Phase portraits of system (1) for $\alpha \in [0.47, 0.8]$.

ogy in each region given in Fig. 1. The complete information for each eigenvalue at different values of α is given in Table 2, where origin and E_2 show the unchanging attitude in their trajectories in all regions, the trajectories around E_1 shows stability in the region $\alpha \in [0.5, 0.55]$ and saddle for $\alpha \in (0.55, 0.8)$. The interesting dynamics has been observed in the equilibrium points E_3 and P, where saddle focus can be seen with a single real and a pair of complex conjugate eigenvalues. Therefore, Table 2 shows that E_3 and P have the best chances of exhibiting Hopf and codimension-two bifurcations. The study of existence of chaos in system (1) is further extended by plotting two-parameter bifurcation diagram and its corresponding Lyapunov exponent in Fig. 4. The region enclosed in a rectangular region with $\alpha = 0.5$ and $c = 10$ shows chaotic region, whereas the other colored regions show periodic solutions.

EP	Stability for different α ranges				
	$\alpha = 0.5$	$\alpha \in (0.5, 0.55)$	$\alpha \in (0.55, 0.6]$	$\alpha \in (0.6, 0.7)$	$\alpha \in (0.7, 0.8)$
O	Saddle $(-10,\ 16.5,\ 30)$	Saddle $(-10,\ 16.5,\ 30)$	Saddle $(-10,\ 16.5,\ 30)$	Saddle $(-10,\ 16.5,\ 30)$	Saddle $(-10,\ 16.5,\ 30)$
E_1	Stable $(-10, -16.5, -3)$	Stable $(-10, -16.5, -1.3)$	Saddle $(-10,\ -16.5,\ 2.5)$	Saddle $(-10,\ -16.5,\ 4.6)$	Saddle $(-10,\ -16.5,\ 8)$
E_2	Saddle $(-30,\ 62.3,\ -55.8)$	Saddle $(-30,\ 62.3,\ -55.8)$	Saddle $(-30,\ 62.3,\ -55.8)$	Saddle $(-30,\ 62.3,\ -55.8)$	Saddle $(-30,\ 62.3,\ -55.8)$
E_3	Saddle focus $\begin{pmatrix} 6.5 \\ -2.1 + 15.9i \\ -2.1 - 15.9i \end{pmatrix}$	Saddle focus $\begin{pmatrix} 6.5 \\ -2.1 + 15.9i \\ -2.1 - 15.9i \end{pmatrix}$	Saddle focus $\begin{pmatrix} 6.5 \\ -2.1 + 15.9i \\ -2.1 - 15.9i \end{pmatrix}$	Saddle focus $\begin{pmatrix} 6.5 \\ -2.1 + 15.9i \\ -2.1 - 15.9i \end{pmatrix}$	Saddle focus $\begin{pmatrix} 6.5 \\ -2.1 + 15.9i \\ -2.1 - 15.9i \end{pmatrix}$
E_4	Saddle $\begin{pmatrix} 2.5 \\ -17.8 \\ -8.1 \end{pmatrix}$	Saddle $\begin{pmatrix} 1.1 \\ -17.1 \\ -9.2 \end{pmatrix}$	Stable $\begin{pmatrix} -3.2 \\ -14.5 \\ -11.9 \end{pmatrix}$	Stable focus $\begin{pmatrix} -14.1 \\ -9.5 + 2.4i \\ -9.5 - 2.4i \end{pmatrix}$	Stable focus $\begin{pmatrix} -18.7 \\ -10.7 + 9.3i \\ -10.7 - 9.2i \end{pmatrix}$
P	Saddle focus $\begin{pmatrix} -13.4 \\ 1.4 + 7.7i \\ 1.4 - 7.7i \end{pmatrix}$	Saddle focus $\begin{pmatrix} -12.9 \\ 1.1 + 8.2i \\ 1.1 - 8.2i \end{pmatrix}$	Saddle focus $\begin{pmatrix} -11.8 \\ 0.6 + 9.1i \\ 0.6 - 9.1i \end{pmatrix}$	Saddle focus $\begin{pmatrix} -11.2 \\ 0.3 + 9.6i \\ 0.3 - 9.6i \end{pmatrix}$	Stable focus $\begin{pmatrix} -10.2 \\ -0.2 + 10.4i \\ -0.2 - 10.4i \end{pmatrix}$

Table 2. Stability conditions of equilibrium points based on eigenvalues.

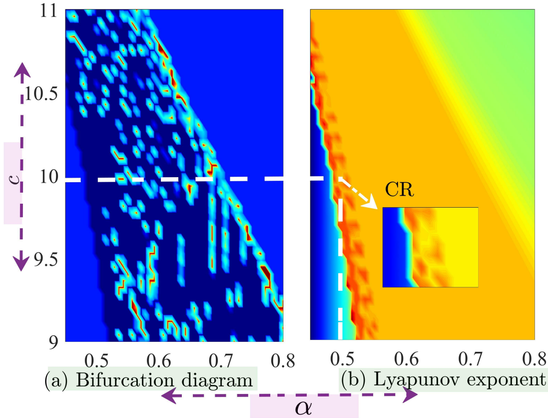

Figure 4. The complete dynamics of system (1) for $\alpha \in [0, 0.8]$ and $c \in [9, 11]$ by plotting its (a) Bifurcation diagram and (b) maximum Lyapunov exponent.

2 Bifurcation analysis in autocatalytic chemical reaction system

In this section, we have used the method derived by Kuznetsov [41] to determine Hopf bifurcation, its type around E_3 and P and extended to generalized Hopf (Bautin) bifurcation. Moreover, the considered system is physically interpreted by showing the impact of Hopf and Bautin bifurcations on it.

2.1 Hopf and Bautin bifurcations at $E_3(c, a - bc, 0)$

We begin with shifting E_3 to origin O

$$\begin{cases} \dot{X} = -((c + X)(bX + Y + Z)), \\ \dot{Y} = X(a - bc + Y), \\ \dot{Z} = -Z(c - d + X + \alpha Z). \end{cases} \tag{3}$$

The characteristic equation of system (3) at $O(0,0,0)$ is

$$h_1(\lambda) = -\lambda^3 + \varphi_2\lambda^2 + \varphi_1\lambda + \varphi_0, \tag{4}$$

where $\varphi_0 = -ac^2+acd+bc^3-bc^2d$, $\varphi_1 = (bcd-ac)$, $\varphi_2 = d-bc-c$. Assume that Eq. (4) has a pair of pure imaginary roots $\lambda_{1,2} = \pm \mathrm{i}\omega$ $(\omega > 0)$, then

$$\begin{cases} \omega^3 + (bcd - ac)\omega = 0, \\ (bc + c - d)\omega^2 - ac^2 + acd + bc^3 - bc^2 d = 0, \end{cases} \tag{5}$$

yielding the bifurcation surface

$$bc\left(ac - (b+2)cd + c^2 + d^2\right) = 0 \tag{6}$$

and

$$\omega = \sqrt{ac - bcd}, \ \text{ where } \ (a - bd)c > 0. \tag{7}$$

For convenience, we further considered $a = c$, $b = 0$, $d = 2c$, $(c > 0)$ to get $\omega = c$ and simplified bifurcation surface (6). As a result of these changing, the Jacobian matrix at the origin become

$$A = \begin{pmatrix} 0 & -c & -c \\ c & 0 & 0 \\ 0 & 0 & d-c \end{pmatrix}. \tag{8}$$

The four vectors, satisfying orthogonality condition[‡]

$$q = \begin{pmatrix} 1 \\ -2\mathrm{i} \\ \mathrm{i} \end{pmatrix}, \overline{q} = \begin{pmatrix} 1 \\ 2\mathrm{i} \\ -\mathrm{i} \end{pmatrix},$$

$$p = \begin{pmatrix} -\frac{(c(1+\mathrm{i})-d\mathrm{i})\mathrm{i}}{\sigma_1} \\ -\frac{c(1+\mathrm{i})-d\mathrm{i}}{\sigma_1} \\ -\frac{c(-3d+c(3+2\mathrm{i}))}{13c^2-18cd+9d^2} \end{pmatrix}, \overline{p} = \begin{pmatrix} \frac{(c(1-\mathrm{i})+d\mathrm{i})\mathrm{i}}{\sigma_1} \\ -\frac{c(1-\mathrm{i})+d\mathrm{i}}{\sigma_1} \\ -\frac{c(-3d+c(3-2\mathrm{i}))}{13c^2-18cd+9d^2} \end{pmatrix},$$

[‡]Orthogonality condition: $\langle p, q\rangle = 1$

where $\sigma_1 = -3d + c(3+2\mathrm{i})$, are derived using $Aq{=}\mathrm{i}\omega q$, $A\bar{q}{=}-\mathrm{i}w\bar{q}$, $A^T p{=}-\mathrm{i}wp$ and $A^T\bar{p}{=}\mathrm{i}w\bar{p}$ [41, Eq. (5.26), page 196]. There is only a bilinear term in the system (3). Therefore the bilinear $B(\xi,\eta)$, defined for two vectors $\xi = (\xi_1,\xi_2,\xi_3)^T \in \mathbb{R}^3$ and $\eta = (\eta_1,\eta_2,\eta_3)^T \in \mathbb{R}^3$, can be expressed as

$$B(\xi,\eta) = \begin{pmatrix} -\xi_1\eta_2 - \xi_2\eta_1 - \xi_1\eta_3 - \xi_3\eta_1 \\ \xi_1\eta_2 + \xi_2\eta_1 \\ -\xi_1\eta_3 - \xi_3\eta_1 - 2\alpha\xi_3 y_3 \end{pmatrix}. \tag{9}$$

Our target is to obtain the value of the first Lyapunov coefficient to determine type of Hopf bifurcation, therefore we compute

$$A^{-1} = \begin{pmatrix} 0 & \frac{1}{c} & 0 \\ -\frac{1}{c} & 0 & \frac{1}{c-d} \\ 0 & 0 & -\frac{1}{c-d} \end{pmatrix}, \quad B(q,q) = \begin{pmatrix} 2\mathrm{i} \\ -4\mathrm{i} \\ 2\alpha - 2\mathrm{i} \end{pmatrix},$$
$$B(q,\overline{q}) \begin{pmatrix} 0 \\ 0 \\ -2\alpha \end{pmatrix}. \tag{10}$$

The inverse of matrix $(2\mathrm{i}\omega E - A)$ at $\omega = c$ gives

$$(2\mathrm{i}\omega E - A)^{-1}|_{\omega=c} = \begin{pmatrix} -\frac{2\mathrm{i}}{3c} & \frac{1}{3c} & \frac{2}{3(c(2-\mathrm{i})+d\mathrm{i})} \\ -\frac{1}{3c} & -\frac{2\mathrm{i}}{3c} & \frac{1}{3(-d+c(1+2\mathrm{i}))} \\ 0 & 0 & \frac{1}{-d+c(1+2\mathrm{i})} \end{pmatrix}. \tag{11}$$

Substituting Eqs. (8-11) into the first Lyapunov coefficient

$$\begin{aligned} \ell_1(0) = & \frac{1}{2\omega}\mathrm{Re}\left[\langle p, C(q,q,\bar{q})\rangle - 2\langle p, B(q, A^{-1}B(q,\bar{q}))\rangle\right. \\ & \left.+\langle p, B(\bar{q},(2i\omega E - A)^{-1}B(q,q))\rangle\right] \end{aligned} \tag{12}$$

yields

$$\ell_1(0) = \frac{168c^5\alpha^2 + 160c^5\alpha + 113c^5 - 144c^4d\alpha^2 - 270c^4d\alpha - 255c^4d}{-195c^7 + 543c^6d - 630c^5d^2 + 390c^4d^3 - 135c^3d^4 + 27c^2d^5} + \frac{72c^3d^2\alpha^2 + 170c^3d^2\alpha + 210c^3d^2 - 66c^2d^3\alpha}{-195c^7 + 543c^6d - 630c^5d^2 + 390c^4d^3 - 135c^3d^4 + 27c^2d^5} + \frac{-94c^2d^3 + 6cd^4\alpha + 29cd^4 - 3d^5}{-195c^7 + 543c^6d - 630c^5d^2 + 390c^4d^3 - 135c^3d^4 + 27c^2d^5}. \tag{13}$$

Proposition 1. *If $\ell_1(0) < 0$, then Hopf bifurcation at the equilibrium E_3 is non-degenerate and supercritical, while $\ell_1(0) > 0$ gives the non-degenerate subcritical Hopf bifurcation at E_3.*

Proposition 2. *For $d = 3.2$, $g = 2.2$, Eq.* (13) *is reduced into a quadratic equation $-1.2234b^2 + 0.9971b - 0.1621$ with critical points b_c=*{0.590723, 0.224301}*. The points in the set b_c exhibits Bautin bifurcation with the second Lyapunov coefficient $\ell_2(0) = -0.0610$, using analytical formula given in [41, Eq. 8.24, p. 344], for $b = 0.590723$ and $\ell_2(0) = 0.1384$ for $b = 0.224301$.*

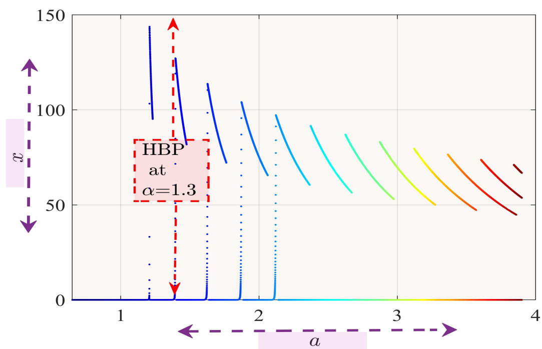

Figure 5. Bifurcation diagram of system (1) showing Hopf bifurcation at the equilibria E_3 for the variations in a.

Moreover, in Proposition 1 the conditions for various signs of Lyapunov coefficient are possible mathematically but the existence of unstable limit cycle in a chemical reaction system can cause unbounded growth or negative concentrations as the reasons for violating physical constraints. Hence,

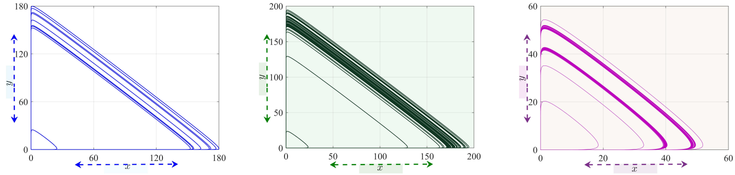

(a) (b) (c)

Figure 6. Hopf bifurcation in system (1) at the equilibria E_3 for (a) less than (b) equals to and (c) greater than Hopf bifurcation parameter; a

consequently the physical interpretation shows impossibility of the bifurcation to be subcritical Hopf bifurcation. In Fig. 5, the Hopf bifurcation parameter is selected in the range of $a \in [0.5, 4]$ which is further explored in Fig. 6, where our considered system is plotted by tuning bifurcation parameter. It has been observed that the trajectories shows convergence describing focus changes into center and two negligible limit cycles elaborating the supercritical case.

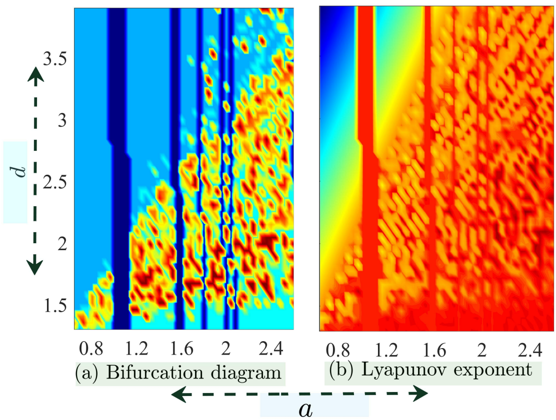

Figure 7. Complete dynamical analysis of system (1) around Hopf bifurcation parameter for $a \in [0, 8.2.4]$ and $d \in [1.2, 3.9]$ by plotting its (a) bifurcation diagram and (b) maximum Lyapunov exponent.

Figure 7 shows the bifurcation diagram and maximum Lyapunov exponent for $a \in [0.5, 2.5]$ and $d \in [1.2, 3.9]$. These two figures give complete dynamics of system around these two parameter values to explore the existence of Bautin bifurcation.

For the physical interpretation of Hopf bifurcation of system (1) at E_3, the real parameter are given in Sect. (1) where $a = k_1 [A_1]$ depends on the reaction rate k_1 and the concentration of species A_1, whereas $d = k_4 [A_4]$ shows dependency on the reaction rate k_4 and the concentration of species A_4. Therefore, the Hopf bifurcation indicates a balance between two key reaction processes i.e. autocatalytic production of X from A_1 such that; $A_1 + X \rightleftharpoons 2X$ and depletion of X through reaction with Z; $X + Z \rightleftharpoons A_3$ dictates the rate at which X is removed.

Finally, at the Hopf bifurcation point $a = d$, these opposing processes are in a delicate balance, leading to the onset of oscillatory behavior. When $a < d$, depletion dominates, and the system remains at a stable steady state. However, as a increases and reaches d, a supercritical Hopf bifurcation occurs, resulting in small-amplitude oscillations that grow as $a > d$, leading to sustained periodic variations in X, Y, and Z. In industrial reactors, controlling $[A_1]$ and $[A_4]$ near $a = d$ is essential to maintain stability for catalytic processes. Thus, this bifurcation highlights the transition between steady-state and dynamic chemical behavior, offering insights into reaction kinetics and pattern formation.

2.2 Hopf and Bautin bifurcations at $P(c, a - bc + \frac{c-d}{\alpha}, \frac{d-c}{\alpha})$

To analyze the Hopf bifurcation of system (1) at the equilibria P, we have to compute the first Lyapunov coefficient $\ell_1(0)$. For this, first we translate P to origin O using the change of variables

$$\begin{cases} x(t) = X(t) + c, \\ y(t) = Y(t) + a - bc + \dfrac{c-d}{\alpha}, \\ z(t) = Z(t) + \dfrac{d-c}{\alpha}. \end{cases} \tag{14}$$

In view of Eq. (14), we get the following equivalent system

$$\begin{cases} \dot{X} = -((c+X)(bX+Y+Z)), \\ \dot{Y} = \frac{X(\alpha(a+Y)-\alpha bc+c-d)}{\alpha}, \\ \dot{Z} = \frac{(X+\alpha Z)(c-d-\alpha Z)}{\alpha}, \end{cases} \tag{15}$$

where X, Y and Z are state variables of the transformed system. The characteristic equation of system (15) at the point $O(0,0,0)$ is

$$h(\lambda) = -\lambda^3 + \Upsilon_2\lambda^2 + \Upsilon_1\lambda + \Upsilon_0, \tag{16}$$

where

$$\begin{aligned} \Upsilon_0 &= ac^2 - acd - bc^3 + bc^2 d + \frac{c^3}{\alpha} - \frac{2c^2 d}{\alpha} + \frac{cd^2}{\alpha}, \\ \Upsilon_1 &= \left(2bc^2 - ac - bcd - \frac{2c^2}{\alpha} + \frac{2cd}{\alpha}\right), \\ \Upsilon_2 &= c - bc - d. \end{aligned}$$

Assume that Eq. (16) has a pair of pure imaginary roots $\lambda_{1,2} = \pm i\omega$ $(\omega > 0)$, which leads to the bifurcation surface

$$\begin{aligned} &c\left(abc\alpha + cd\left(b^2\alpha - 2b(\alpha+1) + 2\right)\right. \\ &\left.- \left((2b-1)c^2(b\alpha - 1)\right) + d^2(b\alpha - 1)\right) = 0 \end{aligned} \tag{17}$$

and

$$\omega = \sqrt{c\left(a + b(d-2c) + \frac{2(c-d)}{\alpha}\right)}, \tag{18}$$

such that $c\left(a + b(d-2c) + \frac{2(c-d)}{\alpha}\right) > 0$. The bifurcation surface (17) seems complex in the presence of a lot of parameters, therefore we consider a special case: $a = \frac{2c}{\alpha} + c$, $b = \frac{1}{2c}$, $d = 2c$, $\alpha = c$, $(c > 0)$. Substituting these values into Eq. (18) and the Jacobian matrix at the origin to obtain

$\omega = c$ and

$$A = \begin{pmatrix} -\frac{1}{2} & -c & -c \\ c + \frac{1}{2} & 0 & 0 \\ -1 & 0 & -c \end{pmatrix}.$$

The four generalized vectors

$$q = \begin{pmatrix} c^2(1-\mathrm{i}) \\ -c\big(c+\frac{1}{2}\big)(1+\mathrm{i}) \\ c\mathrm{i} \end{pmatrix}, \bar{q} = \begin{pmatrix} c^2(1+\mathrm{i}) \\ c\big(c+\frac{1}{2}\big)(-1+\mathrm{i}) \\ -c\mathrm{i} \end{pmatrix}, \tag{19}$$

and

$$p = \begin{pmatrix} \frac{1+\mathrm{i}}{c(4c\mathrm{i}-1+\mathrm{i})} \\ \frac{1-\mathrm{i}}{c(4c\mathrm{i}-1+\mathrm{i})} \\ -\frac{\mathrm{i}}{c(4c\mathrm{i}-1+\mathrm{i})} \end{pmatrix}, \bar{p} = \begin{pmatrix} \frac{-1+\mathrm{i}}{c(4c\mathrm{i}+1+\mathrm{i})} \\ \frac{-1-\mathrm{i}}{c(4c\mathrm{i}+1+\mathrm{i})} \\ -\frac{\mathrm{i}}{c(4c\mathrm{i}+1+\mathrm{i})} \end{pmatrix} \tag{20}$$

are obtained using $Aq{=}\mathrm{i}\omega q$, $A\bar{q}{=}-\mathrm{i}w\bar{q}$, $A^T p{=}-\mathrm{i}wp$ and $A^T\bar{p}{=}\mathrm{i}w\bar{p}$ [41,

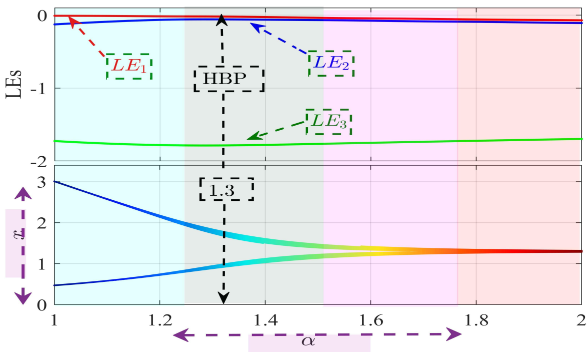

Figure 8. Bifurcation diagram and Lyapunov exponents of system (1) showing Hopf bifurcation at the equilibria P for the variations in α.

Eq. (5.26), page 196] and satisfying orthogonality condition in a complex field. Moreover, the following matrix is calculated

$$(2\mathrm{i}\omega E - A)^{-1}|_{\omega=c} = \begin{pmatrix} \frac{\frac{8}{3}-\frac{4}{3}\mathrm{i}}{1+\sigma_2} & \frac{\frac{2}{3}+\frac{4}{3}\mathrm{i}}{1+\sigma_2} & \frac{4}{3(c(4-2\mathrm{i})-\mathrm{i})} \\ -\frac{\sigma_2+1+2\mathrm{i}}{\sigma_1} & \frac{c(8-4\mathrm{i})+1-2\mathrm{i}}{\sigma_1} & \frac{2c+1}{\sigma_1} \\ \frac{4\mathrm{i}}{\sigma_1} & -\frac{2}{\sigma_1} & \frac{6c-1-2\mathrm{i}}{\sigma_1} \end{pmatrix}, \tag{21}$$

where $\sigma_1{=}3\left(c^2(2+4\mathrm{i})+c\right)$, $\sigma_2{=}c\,(2+4\mathrm{i})$ and

$$A^{-1} = \begin{pmatrix} 0 & \frac{2}{2c+1} & 0 \\ -\frac{1}{c} & \frac{1}{c(2c+1)} & \frac{1}{c} \\ 0 & -\frac{2}{c(2c+1)} & -\frac{1}{c} \end{pmatrix} \tag{22}$$

to achieve the first Lyapunov coefficient using Eq. (12)

$$\ell_1(0) = -\frac{6c^3\left(12c^2+8c+1\right)}{160c^4+112c^3+44c^2+8c+1} < 0. \tag{23}$$

Eq. (23) shows that the Hopf bifurcation of system (1) at the positive

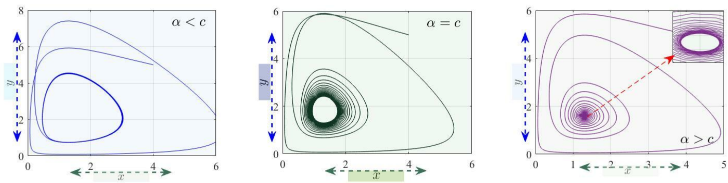

(a) (b) (c)

Figure 9. Hopf bifurcation in system (1) at the positive equilibria at various bifurcation parameter values showing (a) stable focus changes into (b) center leading to (c) unstable focus surrounded by limit cycle.

equilibria P is non-degenerate and supercritical. As $\alpha = k_{\overline{5}}$ represents the reverse reaction rate for $A_4 + Z \rightleftharpoons 2Z$ and $c = k_5\,[A_5]$ shows the rate of depletion in Y due to $A_5 + Y \rightleftharpoons A_2$. Hence, the Hopf bifurcation at $\alpha = c$ suggests that the balancing between these two reaction processes elaborates whether the system remains at a steady state or undergoes sustained oscillations. In Hopf bifurcation, the dynamical system passes from three phases, first at $\alpha < c$ (before the bifurcation point): system (1) has stable focus, meaning that the concentrations of X, Y, Z remain constant over time and corresponds to a region where the autocatalysis in Z is weaker than the depletion of Y. Moving to the bifurcation point $\alpha = c$, the system undergoes a supercritical Hopf bifurcation, leading to the emergence of stable periodic oscillations in the concentrations of X, Y, and Z meaning that the competition between autocatalysis in Z and depletion of Y has reached a threshold where sustained oscillations become energetically favorable. Finally, after the bifurcation point; $\alpha > c$, stable oscillations changes their nature, meaning that the species X, Y, Z will no longer settle down at the equilibria but will instead cycle periodically over time. The increasing effect of autocatalysis in Z dominates over the depletion process c, allowing self-sustained chemical oscillations.

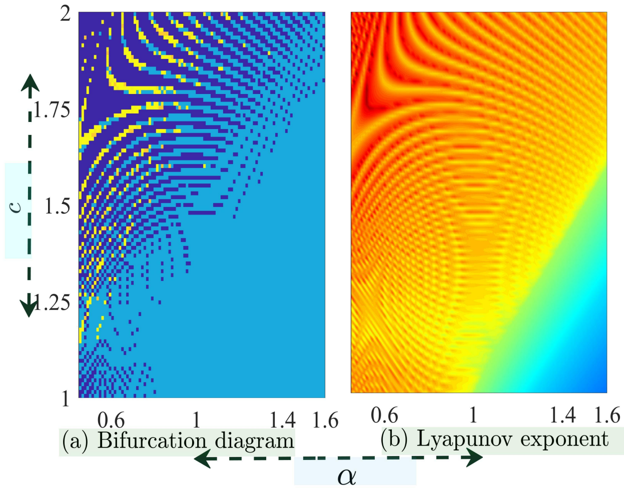

Figure 10. Complete dynamical analysis of system (1) around Hopf bifurcation parameter for $\alpha \in [0, 47.1.6]$ and $c \in [1, 2]$ by plotting its (a) bifurcation diagram and (b) maximum Lyapunov exponent.

Figure 10 shows the bifurcation diagram and Lyapunov exponent that is plotted for the variation in two parameters at a time. For α=c=1.3, there exist Hopf bifurcation and other colors represents various other types of bifurcation around the equilibria P. Hence, Fig. 10 shows a glimpse of other type of bifurcations. Therefore, we extend our study to the point at which Eq. (23) equals to zero i.e. $\ell_1(0) = 0$. Hence, computing $\ell_1(0) = 0$ gives $c = 0$, $c = -\frac{1}{2}$ and $c = -\frac{1}{6}$ in which all the three cases are physically impossible in system (1) due to the reason that $c = k_5\,[\,\mathrm{A}_5]$, where $k_5 > 0$ and $[\mathrm{A}_5] > 0$ that implies c must be positive in any realistic chemical system. But mathematically, the bautin bifurcation is possible for $c = -\frac{1}{6}$ leading to a region where both stable and unstable limit cycles exist, whereas the other two gives that the Jacobian matrix of the considered system is singular. In bautin bifurcation, the analytical formulas given by Kuznetsov et al. [41] are user friendly and easy to use except the computation of h_{21}. The term

$$h_{21} = (i\omega I_3 - A)^{-1}[B(\bar{q}, \bar{h}_{20}) + 2B(qh_{11}) - 2c_1 q] \tag{24}$$

satisfies the orthogonality condition $\langle p, h_{21}\rangle = 0$ and hence can be solved analytically. Now, using Eqs. (17-23) along with Eq. (24) and the formulas given in [41, pp. 343-344] into the second Lyapunov coefficient [41, Eq. 8.24, p. 344] gives $\ell_2(0) = -0.4589$. The $\mathrm{sign}(\ell_2) = -1$, therefore, the truncated normal form for bautin bifurcation of system (1) at the unfolding parameters $\Phi_1 = c$ and $\Phi_2 = \frac{\ell_1(0)}{0.6774}$ is

$$\dot{\Psi} = \Psi\left(\Phi_1 + \Phi_2\Psi^2 - \Psi^4\right),\ \ \dot{\Theta} = 1. \tag{25}$$

These unfolding parameters scales the transition between different oscillatory states, meaning that small perturbations in reaction rates can induce large qualitative changes. The Bautin bifurcation in our chemical system indicates a highly sensitive transition between different oscillatory regimes. The coexistence of multiple oscillatory states implies that small parameter changes (e.g., reaction rates $k_{\overline{5}}$ and $k_5\,[A_5]$) could shift the system between different dynamic behaviors. This has significant implications for reaction stability, biochemical regulation, and chemical pattern formation. In Fig. 8, the bifurcation diagram along with its corresponding Lyapunov exponents, by bringing changing in the bifurcation parameter; α, are given to show the existence of Hopf bifurcation at $\alpha = 1.3$, whereas in Fig. 9, the analytical results given in subsection (2.2) are verified qualitatively. Starting from the parameter value; a less than bifurcation parameter gives a stable focus with all negative Lyapunov exponents that changes into a center with double zero Lyapunov exponents exactly at the bifurcation parameter. Moreover, exceeding the value further a deep and dense black area, with single zero and other negative Lyapunov exponents, is observed that by zooming can illustrate a negligible limit cycle.

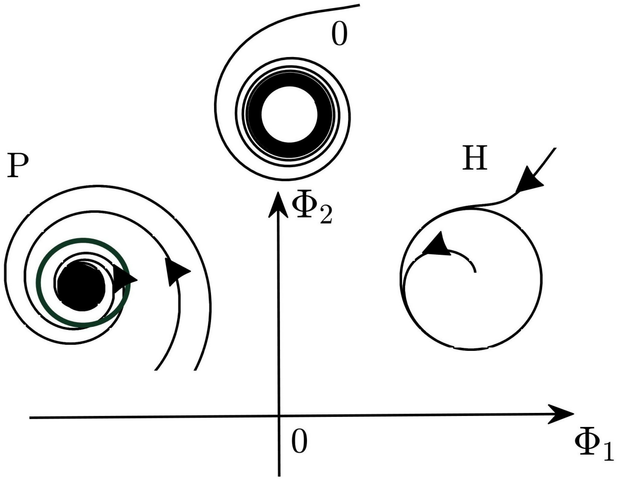

Figure 11. Bautin bifurcation diagram of system (25) with a negative second Lyapunov coefficient i.e. $\text{sign}(\ell_2) = -1$

Figure 11 is the bifurcation diagram of system (25) illustrating bautin bifurcation, where H is for the Hopf bifurcation such that $H = \{(\Phi_1, \Phi_2), \Phi_1 = 0\}$ and $P = \{(\Phi_1, \Phi_2),\ \Phi_2^2 + 4\Phi_1 = 0\}$ shows the semi-parabolic curve. Starting from the point O, a stable spiral emerges where the chemical concentrations of the system decay to steady values with respect to time that changes into a stable limit cycle in the region of H indicating supercritical Hopf bifurcation. Moving further into the region bounded by H and $P\,(\Phi_1 > 0, \Phi_2 > 0)$, the considered system remains oscillatory with a single stable limit cycle and the oscillation amplitude gradually increases as parameters change. Finally, the limit cycle disappears as approaches to the region P with the aid of fold bifurcation.

In a chemical reactor, adjusting Φ_1 and Φ_2, that depend on reaction rates and concentrations can be shifted to the system between stable steady-state and oscillatory reaction dynamics. Moreover, the existence of fold bifurcation of limit cycles identifies that system (1) can switch back to steady behavior even after oscillations. Finally, the appearance and vanishing attitude of limit cycles relate to the spatiotemporal patterns in such systems.

3 Conclusion

Chemical reactions are the fundamental source of combining several objects to create a new one. In some cases, the chemical reactions show unpredictability with a negligible change in experiment pattern. Bifurcations are considered as mini-chaos for such sensitive dynamical models. Therefore, in the current paper some chemical reactions (2) have been combined to create the Williamowski-Rossler system. In the past, it was shown that the considered system has local dynamical behavior for five equilibrium points, whereas the positive equilibria undergoes a numerical Hopf bifurcation. However, in the current paper, some new parametric conditions have been presented for the positive equilibria and E_3 that not only verified Hopf bifurcation but also determined its type and Bautin bifurcation using the first Lyapunov coefficient. In both cases, the bifurcations have been calculated as supercritical and discussed qualitatively in Figs. 9 and 6.

Physically, the Hopf bifurcations at their corresponding bifurcation points mark a critical transition point where the trajectories of a chemical system shifted from a steady to unsteady state oscillations. The balancing between auto-catalysis and depletion were noted important factors to this behavior. Moreover, the Bautin bifurcation in chemical system (1) indicated a highly sensitive transition between various oscillatory regimes. The coexistence of multiple oscillatory states implied that small parameter changes shifted the system between different dynamic behaviors. The adjustment of unfolding parameters in Bautin bifurcation had elaborated a shifting attitude in the considered system between stable steady-state and oscillatory reaction dynamics. In Fig. 11, the complete cycle was described that how the emergence and vanishing of limit cycle can affect the dynamics of our considered dynamical system.

***Acknowledgment*:** Acknowledgment: This work was supported by the National Natural Science Foundation of China, Grant No. 12471166 (F. Li); the Natural Science Foundation of Shandong Province, China, Grant No. ZR2024MA037 (F. Li); Natural Science Foundation of Shandong Province, China, Grant No. ZR2022QA057 (Y. Wei).

Data availability The MATLAB codes will be provided to readers upon a request from the corresponding author.

Declaration of Competing Interest The authors declare that they have no known competing financial interests or personal relationships that could have appeared to influence the work reported in this paper.

References

[1] Q. Din, Dynamics and Hopf bifurcation of a chaotic chemical reaction model, *MATCH Commun. Math. Comput. Chem.* **88** (2022) 351–369.

[2] Q. Din, T. Donchev, D. Kolev, Stability, bifurcation analysis and chaos control in chlorine dioxide–iodine–malonic acid reaction, *MATCH Commun. Math. Comput. Chem.* **79** (2018) 577–606.

[3] M. A. Khan, Q. Din, Codimension-one and codimension-two bifurcations of a fractional-order cubic autocatalator chemical reaction system, *MATCH Commun. Math. Comput. Chem.* **91** (2024) 415–452.

[4] M. X. Chen, Hopf Bifurcation and self-organization pattern of a modified Brusselator model, *MATCH Commun. Math. Comput. Chem.* **90** (2023) 581–607.

[5] M. A. Khan, M. S. Khan, Q. Din, Codimension-one and codimension-two bifurcations of a modified Brusselator model, *Int. J. Dyn. Control* **13** (2025) #154.

[6] Q. Din, U. Saeed, Stability, discretization, and bifurcation analysis for a chemical reaction system, *MATCH Commun. Math. Comput. Chem.* **90** (2023) 151–174.

[7] H. L. Smith, Global dynamics of the smallest chemical reaction system with Hopf bifurcation, *J. Math. Chem.* **50** (2012) 989–995.

[8] M. Izadi, H. Ahmad, H. M. Srivastava, Numerical computations of time-dependent auto-catalytic glycolysis chemical reaction-diffusion system, *MATCH Commun. Math. Comput. Chem.* **93** (2025) 69–97.

[9] S. ur Rahman, J. L. Díaz Palencia, J. Roa González, Analysis, symmetry and asymptotic behaviour of solutions for the Belousov-Zhabotinsky model, *MATCH Commun. Math. Comput. Chem.* **93** (2025) 187–222.

[10] Q. Din, M. S. Shabbir, M. A. Khan, A cubic autocatalator chemical reaction model with limit cycle analysis and consistency preserving discretization, *MATCH Commun. Math. Comput. Chem.* **87** (2022) 441–462.

[11] C. Xu, C. Aouiti, Z. Liu, P. Li, L. Yao, Bifurcation caused by delay in a fractional-order coupled oregonator model in chemistry, *MATCH Commun. Math. Comput. Chem.* **88** (2022) 371–396.

[12] R. Wu, L. Yang, Bogdanov-Takens bifurcation of an enzyme-catalyzed reaction model, *Nonlin. Dyn.* **112** (2024) 14363–14377.

[13] M. X. Chen, J. Kim, S. Ham, Patterns of a general chemical model involving Degn-Harrison reaction scheme, *MATCH Commun. Math. Comput. Chem.* **93** (2025) 267–290.

[14] P. Geysermans, G. Nicolis, Thermodynamic fluctuations and chemical chaos in a well-stirred reactor: A master equation analysis, *J. Chem. Phys.* **99** (1993) 8964–8969.

[15] Y. Huang, X. S. Yang, Chaoticity of some chemical attractors: a computer-assisted proof, *J. Math. Chem.* **38** (2005) 107–117.

[16] C. Xu, Y. Wu, Bifurcation and control of chaos in a chemical system, *Appl. Math. Model.* **39** (2015) 2295–2310.

[17] P. Gaspard, Stochastic approach to entropy production in chemical chaos, *Chaos* **30** (2020) #113103.

[18] P. Muthukumar, N. R. Babu, P. Balasubramaniam, Detecting critical point of fractional-order chemical system with synchronization and application to image enhancement technique, *Proc. Natl. Acad. Sci. India Sect. A Phys. Sci.* **91** (2021) 661–674.

[19] A. Allahem, A. Karthikeyan, M. Varadharajan, K. Rajagopal, Computational model of a fractional-order chemical reactor system and its control using adaptive sliding mode control, *Fractals* **30** (2022) 2240243.

[20] H. Wang, Suppressing chaos for a fractional-order chaotic chemical reaction model via PDζ controller, *J. Math.* **2022** (2022) #5658680.

[21] Q. Din, Dynamics and Hopf bifurcation of a chaotic chemical reaction model, *MATCH Commun. Math. Comput. Chem.* **88** (2022) 351–369.

[22] H. Zhou, L. Yang, Dynamical analysis arising from the Willamowski-Rössler model, *J. Math. Anal. Appl.* **514** (2022) #126281.

[23] Z. Liu, Bifurcation anti-control tactics of a fractional-order stable chemical reaction system, *MATCH Commun. Math. Comput. Chem.* **132** (2023) 272–301.

[24] Y. M. Chu, T. Alzahrani, S. Rashid, H. Alhulayyil, W. Rashidah, S. ur Rehman, Complex dynamical analysis of fractional differences Willamowski–Rössler chemical reaction model in time-scale analysis, *Res. Phys.* **54** (2023) #107023.

[25] A. V. Doroshin, N. A. Elisov, Multi-rotor spacecraft attitude control by triggering chaotic modes on strange chaotic attractors, *Nonlin. Dyn.* **112** (2024) 4617–4649.

[26] L. Li, Z. Chai, Y. Wang, A 4-D four-wing chaotic system with widely chaotic regions and multiple transient transitions, *Analog Integr. Circuits Signal Process.* **119** (2024) 195–213.

[27] T. Chen, F. Li, P. Yu, Nilpotent center conditions in cubic switching polynomial Liénard systems by higher-order analysis, *J. Diff. Eq.* **379** (2024) 258–289.

[28] S. Cang, L. Wang, Y. Zhang, Z. Wang, Z. Chen, Bifurcation and chaos in a smooth 3D dynamical system extended from Nose-Hoover oscillator, *Chaos Solitons Fract.* **158** (2022) #112016.

[29] M. O. Al-Kaff, H. A. El-Metwally, A. E. A. Elsadany, E. M. Elabbasy, Exploring chaos and bifurcation in a discrete prey-predator based on coupled logistic map, *Sci. Rep.* **14** (2024) #16118.

[30] F. Li, T. Chen, Y. Liu, P. Yu, A complete classification on the center-focus problem of a generalized cubic Kukles system with a nilpotent singular point, *Qual. Theory Dyn. Syst.* **23** (2024) #8.

[31] M. X. Chen, X. Z. Li, Stability analysis and turing pattern of an enzyme-catalyzed reaction model, *MATCH Commun. Math. Comput. Chem.* **94** (2025) 195–214

[32] X. Y. Zhao, X.Z. Li, M. X. Chen, Spatiotemporal oscillations of an enzyme-catalyzed model, *MATCH Commun. Math. Comput. Chem.* **94** (2025) 605–631.

[33] L. Fan, B. Sang, J. Liu, C. Wang, X. Liu, N. Wang, B. F. Boui A Boya, Bifurcation patterns in some chameleon systems, *Int. J. Bif. Chaos* **34** (2024) #2450149.

[34] Y. Xu, Y. Yang, F. Meng, S. Ruan, Degenerate codimension-2 cusp of limit cycles in a Holling Tanner model with harvesting and anti-predator behavior, *Nonlin. Anal. Real World Appl.* **76** (2024) #103995.

[35] W. Cui, Y. Zhao, Saddle-node bifurcation and Bogdanov-Takens bifurcation of a SIRS epidemic model with nonlinear incidence rate, *J. Diff. Eq.* **384** (2024) 252–278.

[36] H. Chiba, A Hopf bifurcation in the Kuramoto-Daido model, *J. Diff. Eq.* **280** (2021) 546–570.

[37] J. Ma, W. Ren, X. Zhan, Complexity dynamics and Hopf bifurcation analysis based on the first Lyapunov coefficient about 3D IS-LM macroeconomics system, *Commun. Nonlin. Sci. Num. Simul.* **45** (2017) 129–139.

[38] L. Zhou, A. Kabbah, Hopf bifurcation and its control in a 3D autonomous system, *Eur. Phys. J. Spec. Top.* **231** (2022) 2115–2124.

[39] R. Wu, X. Li, Hopf bifurcation analysis and anti-control of Hopf circles of the Rössler-like system, *Abstr. Appl. Anal.* **2012** (2012) #341870.

[40] F. Li, M. Marwan, K. Karawanich, On the bifurcations in a quadrotor unmanned aerial vehicle dynamical system using normal form theory, *Nonlin. Dyn.* **113** (2024) 6405–6425.

[41] Y. A. Kuznetsov, Iu. A. Kuznetsov, Y. Kuznetsov, *Elements of Applied Bifurcation Theory*, Springer, New York, 1998.

[42] J. Zhang, C. Yandong, D. Wenju, C. Yingxiang, A. Xinlei, Hopf bifurcation analysis in a new chaotic system with chaos entanglement function, *J. Appl. Math.* **2014** (2014) #371509.

[43] M. Marwan, S. Ahmad, Bifurcation analysis for energy transport system and its optimal control using parameter self-tuning law, *Soft Comput.* **24** (2020) 17221–17231.

[44] X. Shi, Y. Yang, X. Dai, C. Xiang, Y. Feng, Andronov-Hopf and Bogdanov-Takens bifurcations in a Filippov Hindmarsh-Rose system with switching policy for the slow variable, *Physica D.* **466** (2024) #134217.

[45] X. Yang, M. Yang, H. Liu, X. Liao, Bautin bifurcation in a class of two-neuron networks with resonant bilinear terms, *Chaos Soliton Fract.* **38** (2008) 575–589.

[46] V. G. Inozemtsev, T. A. Tibilov, Lyapunov-Bautin bifurcation and the hunting of a railway wheelset, in: F. L. Chernousko, A. L. Fradkov (Eds.), *2nd International Conference Control of Oscillations and Chaos*, IEEE Xplore, 2000, pp. 279–280.

[47] X. Liu, S. Liu, Codimension-two bifurcation analysis in two-dimensional Hindmarsh–Rose model, *Nonlin. Dyn.* **67** (2012) 847–857.

[48] L. Russo, K. Spiliotis, F. Giannino, S. Mazzoleni, C. Siettos, Bautin bifurcations in a forest-grassland ecosystem with human-environment interactions, *Sci. Rep.* **9** (2019) #2665.